Phenoxyl Radical Complexes of Gallium, Scandium, Iron and Manganese

Britta Adam, Eckhard Bill, Eberhard Bothe, Beatrix Goerdt, Gabriele Haselhorst, Knut Hildenbrand, Achim Sokolowski, Steen Steenken, Thomas Weyhermüller and Karl Wieghardt*

Abstract: The hexadentate macrocyclic ligands 1,4,7-tris(3,5-dimethyl-2-hydroxybenzyl)-1,4,7-triazacyclononane ($L^{CH_3}H_3$), 1,4,7-tris(3,5-di-*tert*-butyl-2-hydroxybenzyl)-1,4,7-triazacyclononane ($L^{Bu}H_3$) and 1,4,7-tris(3-*tert*-butyl-5-methoxy-2-hydroxybenzyl)-1,4,7-triazacyclononane ($L^{OCH_3}H_3$) form very stable octahedral neutral complexes LM^{III} with trivalent (or tetravalent) metal ions (Ga^{III}, Sc^{III}, Fe^{III}, Mn^{III}, Mn^{IV}). The following complexes have been synthesized: $[L^{Bu}M]$, where M = Ga (**1**), Sc (**2**), Fe (**3**); $[L^{Bu}Mn^{IV}]PF_6$ (**4′**); $[L^{OCH_3}M]$, where M = Ga (**1a**), Sc (**2a**), Fe (**3a**); $[L^{OCH_3}Mn^{IV}]PF_6$ (**4a′**); $[L^{CH_3}M]$, where M = Sc (**2b**), Fe (**3b**), Mn^{III} (**4b**); $[L^{CH_3}Mn^{IV}]_2(ClO_4)_3(H_3O)(H_2O)_3$ (**4b′**). An electrochemical study has shown that complexes **1**, **2**, **3**, **1a**, **2a** and **3a** each display three reversible, ligand-centred, one-electron oxidation steps. The salts $[L^{OCH_3}Fe^{III}]ClO_4$ and $[L^{OCH_3}Ga^{III}]ClO_4$ have been isolated as stable crystalline materials. Electronic and EPR spectra prove that these oxidations produce species containing one, two or three coordinated phenoxyl radicals. The Mössbauer spectra of **3a** and $[\mathbf{3a}]^+$ show conclusively that both compounds contain high-spin iron(III) central ions. Temperature-dependent magnetic susceptibility measurements reveal that **3a** has an $S = 5/2$ and $[\mathbf{3a}]^+$ an $S = 2$ ground state. The latter is attained through intramolecular antiferromagnetic exchange coupling between a high-spin iron(III) ($S_1 = 5/2$) and a phenoxyl radical ($S_2 = 1/2$) ($H = -2JS_1S_2$; $J = -80\ cm^{-1}$). The manganese complexes undergo metal- and ligand-centred redox processes, which were elucidated by spectroelectrochemistry; a phenoxyl radical Mn^{IV} complex $[Mn^{IV}L^{OCH_3}]^{2+}$ is accessible.

Keywords
gallium · iron · scandium · spectroelectrochemistry · manganese · phenoxyl radicals

Introduction

A persistent, not coordinatively bound, tyrosyl radical has been unequivocally characterized in the active site of the R2 subunit of the non-heme diiron enzyme ribonucleotide reductase from *Escherichia coli*.[1] This organic radical is located in the vicinity of the oxo-bridged diiron centre, approximately 5.3 Å away from the next nearest iron ion. The spin of this radical ($S = 1/2$) is virtually uncoupled from the spins of the high-spin iron(III) ions, which are strongly antiferromagnetically coupled through a superexchange pathway within the Fe–O–Fe moiety. This ensemble has recently been successfully modelled by a low molecular weight complex.[2]

In contrast, a *coordinated* tyrosyl radical has been discovered in the active form of the copper(II)-containing fungal enzyme galactose oxidase.[3] Owing to the strong intramolecular antiferromagnetic coupling of the tyrosyl radical ligand with the unpaired electron of the Cu^{II} ion (d^9), the active form of the enzyme is diamagnetic and, consequently, EPR-inactive. One-electron reduction of the active site yields an inactive form which displays an EPR spectrum typical for five-coordinate Cu^{II} ions.[3] This form has been structurally characterized by X-ray crystallography.[4] Recently, a new enzyme containing a similar active site with a Cu^{II}-coordinated tyrosyl radical has been described, namely, glyoxal oxidase from *Phanerochaet chrysosporium*.[5]

The coordination chemistry of phenoxyl radicals bound to transition metal ions is not well developed,[6] despite the fact that there are some intriguing problems concerning their electronic structure. In principle, a one-electron oxidation of a transition metal phenolato complex can be either *metal-* or *ligand-*centred (Scheme 1). The question then arises whether the above

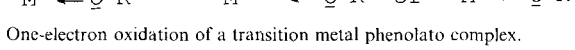

Scheme 1. One-electron oxidation of a transition metal phenolato complex.

two formulations are merely resonance structures of the same electronic ground state, or whether we are dealing with two distinct chemical species with different ground states and different physical and chemical properties.

[*] K. Wieghardt, B. Adam, E. Bill, E. Bothe, B. Goerdt, G. Haselhorst, K. Hildenbrand, A. Sokolowski, S. Steenken, T. Weyhermüller
Max-Planck-Institut für Strahlenchemie, Stiftstrasse 34–36
D-45470 Mülheim an der Ruhr (Germany)
Fax: Int. code +(208)306-3952
e-mail: wieghardt@mpi-muelheim.mpg.de

0947-6539/97/0302-0308 $ 15.00+.25/0

To address questions of this kind experimentally, we have investigated intensively octahedral transition metal complexes containing ligands of the type 1,4,7-tris(*o*-hydroxybenzyl)-1,4,7-triazacyclononane (LH_3).[7, 8] We and others[9, 10] have shown in the past that its trianionic form, $[L]^{3-}$, generates extremely stable[11, 12] neutral complexes [ML] with a number of trivalent metal ions (Table 1).

Table 1. Complexes studied in this paper.

Ligands:

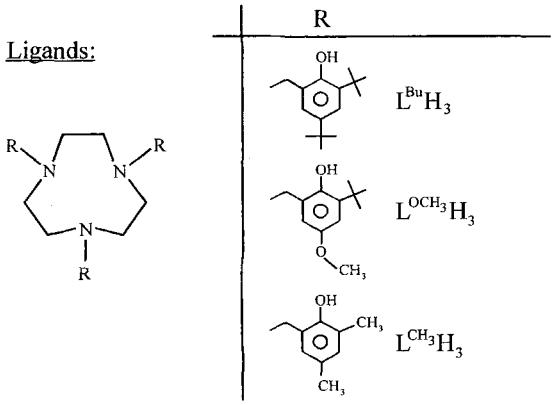

Metal	$L^{tBu}M$	$L^{OCH_3}M$	$L^{CH_3}M$
Ga^{III}	**1**	**1a**	
Sc^{III}	**2**	**2a**	**2b**
Fe^{III}	**3**	**3a**	**3b**
Mn^{III}			**4b**
Mn^{IV}	**4′**	**4a′**	**4b′**

As we will show here, suitable substituents at the *ortho*- and *para*-positions of the pendent *o*-hydroxybenzyl groups of $[L]^{3-}$ facilitate one-electron oxididation to the corresponding phenoxyl radicals. If the substituents are sterically bulky, the radical stability is increased to the extent that they become isolable and spectroscopically characterizable both in solution and in the solid state.

We have recently characterized the neutral complex $[L^{OCH_3}Cr^{III}]$ and its one-electron oxidized form $[L^{OCH_3}Cr^{III}]ClO_4$ by X-ray crystallography. $[L^{OCH_3}Cr^{III}]^+$ has been shown to contain two coordinated phenolate groups and one coordinated phenoxyl radical; the central metal ion is chromium(III).[13]

Results

1. Syntheses: The reaction of 1,4,7-triazacyclononane with three equivalents of di-2,4-*tert*-butylphenol, 2-*tert*-butyl-4-methoxyphenol or 2,4-dimethylphenol with three equivalents of paraformaldehyde in methanol (Mannich reaction) afforded the pendent-arm macrocycles $L^{tBu}H_3$, $L^{OCH_3}H_3$ and $L^{CH_3}H_3$[9] (Table 1) in satisfactory yields as colourless solids. By using $(CD_2O)_n$ and deuterated solvents (CH_3OD, conc. DCL, D_2O) the six benzylic protons of the ligands $L^{tBu}H_3$ and $L^{OCH_3}H_3$ were quantitatively exchanged for deuterium atoms.

The ligands reacted with one equivalent of $GaCl_3$ or $ScCl_3 \cdot 6H_2O$ in refluxing acetonitrile, to which a few drops of triethylamine had been added, to give the neutral complexes $[LM^{III}]$ (Table 1)—colourless **1**, **1a** and colourless to pale yellow **2**, **2a** and **2b**. Complexes deuterated at the benzylic positions complexes $[D_6]$-**1** and $[D_6]$-**2** were obtained analogously by using the deuterated ligands. Slow recrystallization of these complexes from hot CH_3CN solutions produced crystals with two molecules of acetonitrile of crystallization per formula unit. The corresponding reactions with $Fe^{III}(ClO_4)_3 \cdot 9H_2O$ in acetone or CH_3OH produced crystalline red **3**, **3a** and **3b**, respectively. Slow recrystallization from hot CH_3CN again afforded the bis(acetonitrile) species. The solvent molecules evaporated slowly on storage in air. For all subsequent spectroscopic and electrochemical investigations, samples of the complexes dried in vacuo were used.

A mixture of three equivalents of $L^{CH_3}H_3$ and $[Mn^{III}_3(\mu_3\text{-}O)(CH_3CO_2)_6](CH_3CO_2)$ in acetone, to which a few drops of NEt_3 had been added, produced a deep green solution. Upon addition of water a green precipitate of $[Mn^{III}L^{CH_3}]$ (**4b**) was obtained. Slow recrystallization from CH_3OH yielded green crystals of **4b**$\cdot 2CH_3OH$, which were suitable for X-ray crystallography (see below). Acidification of a methanol solution of **4b** with a few drops of concentrated $HClO_4$ in the presence of air resulted in the precipitation of green microcrystals of $[Mn^{IV}L^{CH_3}]_2(ClO_4)_3(H_3O)(H_2O)_3$ ($[\mathbf{4b'}]_2(ClO_4)_3(H_3O)(H_2O)_3$). The presence of the acidic proton was established by potentiometric titration of an aqueous solution of $[\mathbf{4b'}](ClO_4)_3(H_3O)(H_2O)_3$ with 0.10 M NaOH.

Finally, one-electron oxidation of **1a** and **3a** dissolved in dry acetonitrile with one equivalent of $[Ni^{III}(tacn)_2](ClO_4)_3$[14] (tacn = 1,4,7-triazacyclononane) afforded green microcrystals of $[L^{OCH_3}Ga^{III}]ClO_4$ ($[\mathbf{1a}]ClO_4$) and blue crystals of $[L^{OCH_3}Fe]ClO_4$ ($[\mathbf{3a}]ClO_4$) [Eq. (1)].

$$\mathbf{1a}\ (\mathbf{3a}) + [Ni^{III}(tacn)_2](ClO_4)_3 \longrightarrow [\mathbf{1a}]ClO_4([\mathbf{3a}]ClO_4) + [Ni^{II}(tacn)](ClO_4)_2 \quad (1)$$

2. Crystal structures: The crystal structures of the ligands $L^{tBu}H_3$ and $L^{OCH_3}H_3$ have been determined by single-crystal X-ray crystallography, as have the structures of the complexes **2a**, **2b**$\cdot 2CH_3CN$ and **4b**$\cdot 2CH_3OH$; Figures 1–5 show the structures, and Table 2 summarizes important bond lengths and angles of the N_3O_3M coordination polyhedra. The structures

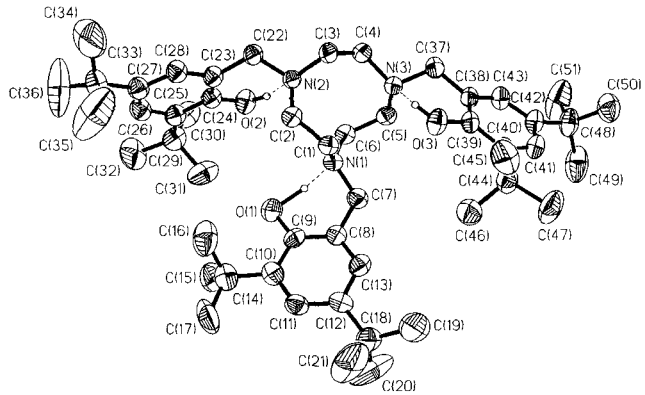

Figure 1. Structure of the ligand $L^{tBu}H_3$. Intramolecular O–H···N contacts [Å]: O(1)···N(1) 2.623(5), O(2)···N(2) 2.716(6), O(3)···N(3) 2.726(6).

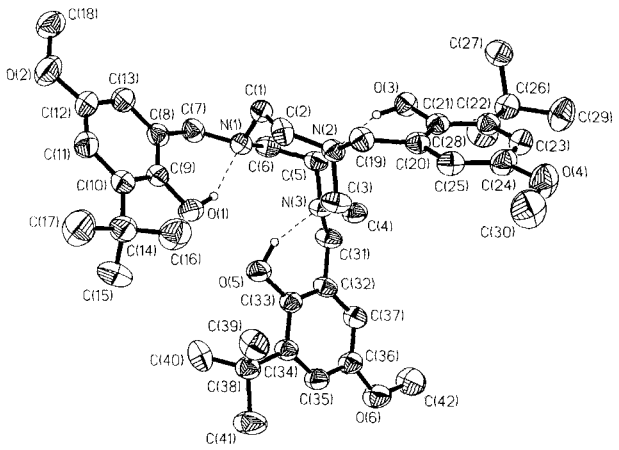

Figure 2. Structure of the ligand $L^{OCH_3}H_3$. Intramolecular O–H···N contacts [Å]: O(1)···N(1) 2.711(5), O(3)···N(2) 2.650(5), O(5)···N(3) 2.647(5).

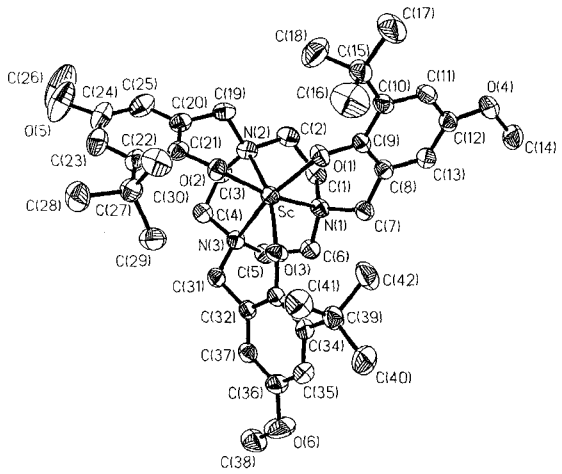

Figure 3. Structure of the neutral complex **2a**.

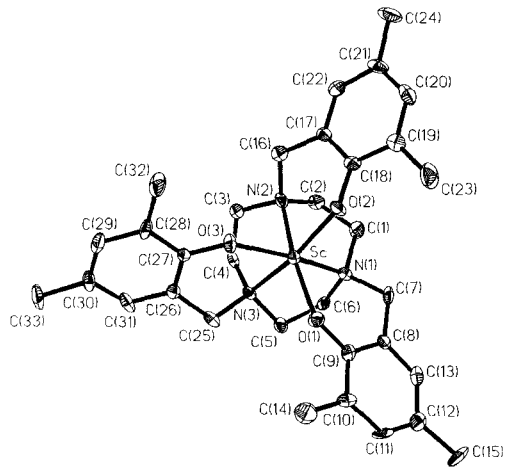

Figure 4. Structure of the neutral complex **2b**.

of $L^{CH_3}H_3$ and of its monoprotonated gallium complex $[L^{CH_3}HGa^{III}]ClO_4 \cdot CH_3OH$ have been determined previously,[9] as have the structures of $[LV]ClO_4$[7c] and of three similar neutral iron(III) complexes.[7a, 7b, 10b]

The structures of the uncoordinated ligands LH_3 (Figures 1 and 2) are very similar, irrespective of the nature of the substituents at the phenyl groups. Each structure consists of neutral LH_3 molecules with three intramolecular N···H–O hydrogen bonding contacts between the tertiary amine nitrogen atoms of the 1,4,7-triazacyclononane ring and the three phenol groups.

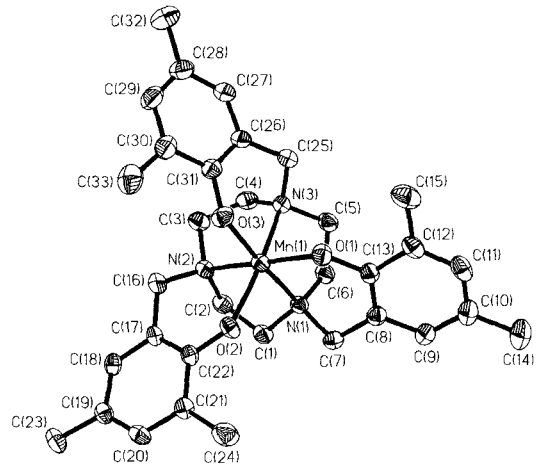

Figure 5. Structure of the neutral complex **4b**.

Table 2. Selected bond lengths [Å] and angles [deg] of complexes.

	[2a]	[2b]·2CH$_3$CN	[4b](CH$_3$OH)$_2$	[4b]$_2$(ClO$_4$)$_3$(H$_2$O)$_3$(H$_3$O)
M–N1	2.354(2)	2.339(8)	2.079(2)	2.04(1)
M–N2	2.365(2)	2.351(6)	2.179(3)	
M–N3	2.412(2)	2.328(9)	2.230(3)	
M–O1	1.977(2)	1.969(5)	1.924(3)	1.83(1)
M–O2	1.977(2)	1.965(8)	2.053(3)	
M–O3	1.960(2)	1.979(7)	1.863(2)	
av. C–O$_{phenolate}$	1.335(3)	1.335(10)	1.345(5)	1.36(2)
O1-M-O2	106.1(1)	105.0(3)	100.9(1)	95.1(2)
O1-M-O3	102.3(1)	106.9(3)	93.1(1)	
O2-M-O3	100.3(1)	105.2(3)	95.1(1)	
N1-M-N2	75.6(1)	75.1(3)	82.1(1)	84.8(4)
N2-M-N3	72.6(1)	75.7(3)	78.8(1)	
N1-M-N3	72.7(1)	75.6(3)	82.1(1)	
O1-M-N1	81.4(1)	83.6(2)	89.5(1)	87.5(3)
O2-M-N2	82.9(1)	82.6(3)	86.9(1)	
O2-M-N3	100.2(1)	156.9(2)	164.8(1)	
O1-M-N3	153.7(1)	92.5(3)	92.5(1)	
O2-M-N1	158.4(1)	91.2(3)	90.7(1)	
O3-M-N2	155.4(1)	90.9(3)	94.4(1)	
O3-M-N1	99.0(1)	157.0(3)	173.0(1)	172.0(3)
O3-M-N3	82.8(1)	83.4(3)	91.3(1)	
O1-M-N2	96.9(1)	157.5(3)	168.6(1)	

The structural analyses of complexes **2a**, [**2b**]·2CH$_3$CN and [**4b**]·2CH$_3$OH (Figures 3–5) confirm that the trianionic ligands are hexadentate and give rise to a facial N_3O_3 donor set. The resulting polyhedron is in all three cases a distorted octahedron with long M–N and comparatively short M–O bond lengths. Interestingly, in **4b** the Mn–O and Mn–N distances are not equivalent. The high-spin d^4-configurated Mn^{III} ion displays a Jahn–Teller tetragonal distortion since the mutually *trans* Mn–N(3) and Mn–O(2) distances are significantly longer than those of the other two axes. Thus, in this case the electronic structure of the central Mn ion determines the geometry of the MnN_3O_3 polyhedron and allows an unambiguous assignment of the oxidation state of the metal ion. The phenolate oxygen O(2) forming the weakest (longest) bond to the Mn^{III} ion forms an O–H···O hydrogen bonding contact to a methanol solvent molecule [O(2)···O(4) 2.825(7) Å].

0947-6539/97/0302-0310 $ 15.00+.25/0 Chem. Eur. J. 1997, 3, No. 2

We have also obtained a low-quality crystal structure of $[\mathbf{4b'}]_2(ClO_4)_3(H_3O)(H_2O)_3$, details of which will be published elsewhere.[15] The structure consists of the monocations $[Mn^{IV}L^{CH_3}]^+$, perchlorate anions and disordered water molecules of crystallization. Charge considerations necessitate the presence of one proton for two Mn^{IV} ions. Since $[\mathbf{4b'}]^+$ is the oxidized form of **4b** it is appropriate to comment on some geometric features of the $[Mn^{IV}L^{CH_3}]^+$ cation. The three Mn–N and Mn–O distances of 2.04(1) and 1.83(1) Å, respectively, are equivalent and significantly shorter than the corresponding bond lengths in the neutral complex $[\mathbf{4b}]\cdot 2CH_3OH$. These data confirm that the one-electron oxidation of **4b** is metal-centred, yielding an octahedral Mn^{IV} (d^3) complex. The Mn^{IV}–O bonds are very short and indicate considerable double-bond character. Consequently, these phenolate oxygen atoms are not involved in hydrogen-bonding contacts to the water molecules or to the H_3O^+ cation.

3. Electrochemistry: The electrochemistry of the complexes has been studied by cyclic voltammetry (CV), square-wave voltammetry and coulometry in acetonitrile solutions containing 0.10 M tetra-*n*-butylammonium hexafluorophosphate as supporting electrolyte; ferrocene was added as internal standard. In the following, all redox potentials are referenced versus the ferrocenium/ferrocene couple (Fc^+/Fc). Table 3 summarizes the measured potentials.

Table 3. Redox potentials [a] of complexes.

	$E^1_{1/2}$ [b]	$E^2_{1/2}$	$E^3_{1/2}$	$E^4_{1/2}$	$E^5_{1/2}$
1	0.87	0.62	0.35		
1a	0.43	0.23	0.01		
2	1.04	0.76	0.52		
2a	0.69	0.47	0.27		
2b		0.80 (irr.)	0.60 (irr.)		
3	0.96 (irr.)	0.65	0.38	−1.78	
3a	0.63	0.38	0.14	−1.81	
3b	1.02 (irr.)	0.84 (irr.)	0.52 (irr.)	−1.58	
4'				−0.43	−0.82
4a'	0.89 (irr.)	0.74 (irr.)	0.56	−0.55	−0.92
4b/4b'				−0.265	−0.85
$[L^{OCH_3}Co^{III}]$ [c]	0.43	0.18	−0.10		
$[L^{OCH_3}Cr^{III}]$ [d]	0.45	0.24	−0.03		

[a] Conditions: [complex] $\approx 10^{-3}$ M in CH_3CN (0.10 M $[N(n\text{Bu})_4]PF_6$), Ar atmosphere, T = 298 K, glassy carbon working electrode; reference electrode Ag/AgCl (saturated LiCl in C_2H_5OH); ferrocene internal standard; scan rate: 200 mVs^{-1}. [b] The potentials are referenced versus the ferrocenium/ferrocene (Fc^+/Fc) couple: $E^x_{1/2} = (E^{ox}_p + E^{red}_p)/2$ for reversible one-electron transfer processes; oxidation peak potentials, E^{ox}_p, are given for irreversible (irr.) processes. [c] Ref. [16]. [d] Ref. [17].

Complexes **1**, **1a** and **2**, **2a**, **2b** contain redox-inactive trivalent Ga^{III} and Sc^{III} ions, respectively. The observed two irreversible oxidation waves in the CV of **2b** shown in Figure 6a must, therefore, be assigned to ligand-centred processes. It is gratifying that the introduction of sterically more demanding *tert*-butyl groups in the *ortho* and *para* positions of the ligands in **2** instead of the methyl groups in **2b** leads to a CV which exhibits *three reversible* one-electron transfer waves.(Figure 6b). Exactly the same electrochemical behaviour is detected for the corresponding gallium complex **1** which also displays three reversible one-electron transfer waves. The three one-electron oxidations of **1** and **2** are assigned to the successive formation of

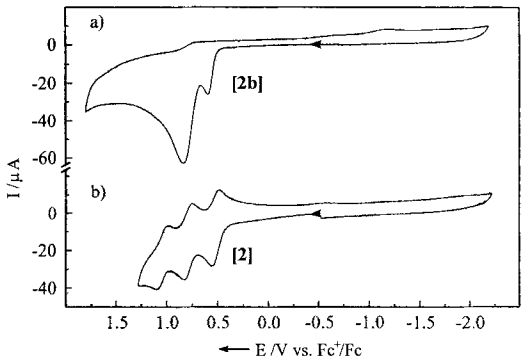

Figure 6. Cyclic voltammograms of **2b** (top) and **2** (bottom) in CH_3CN (0.10 M $[N(n\text{Bu})_4]PF_6$ at a glassy carbon electrode; scan rate: 200 mVs^{-1}; [complex] $\approx 10^{-3}$ M; 298 K).

one, two and three coordinated phenoxyl radicals [Eq (2); M = Ga, Sc].

$$[M^{III}L] \underset{+e}{\overset{-e(E^3)}{\rightleftharpoons}} [M^{III}L]^+ \underset{+e}{\overset{-e(E^2)}{\rightleftharpoons}} [M^{III}L]^{2+} \underset{+e}{\overset{-e(E^1)}{\rightleftharpoons}} [M^{III}L]^{3+} \quad (2)$$

On the timescale of a coulometric experiment at ambient temperature only the monocations $[GaL^{Bu}]^+$ and $[ScL^{Bu}]^+$ are stable. Thus, oxidation of **1** and **2** by one electron equivalent at a constant potential of 0.55 V vs Fc^+/Fc produces yellow-green solutions of the respective monocations, whose UV/Vis spectra (see below) remain unchanged for hours. The di- and trications are unstable under these conditions.

In order to make such phenoxyl radicals more accessible by introducing more easily oxidizable phenolate pendent arms, we prepared the ligand $[L^{OCH_3}]^{3-}$ and its colourless Ga^{III} and Sc^{III} complexes **1a** and **2a**. Figure 7b shows the CV of **2a** and Figure 7a a square-wave voltammogram of **1a**. Again, three reversible one-electron oxidation waves are observed in each case.

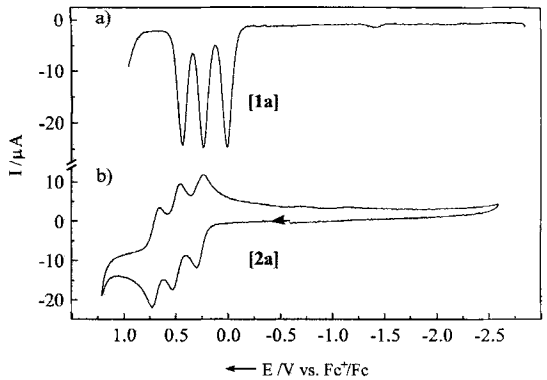

Figure 7. Cyclic voltammogram of **2a** in CH_3CN (conditions as given in Figure 6) and square-wave voltammogram of **1a** in CH_3CN (0.10 M $[N(n\text{Bu})_4]PF_6$; frequency: 30 Hz; pulse height 2.5×10^{-2} V; glassy carbon electrode).

The stability of both monocations in solution at ambient temperature is excellent. The redox potentials of **1a** and **2a** are shifted by ≈350–410 mV to less positive potentials compared to those of **1** and **2**. The corresponding di- and trications of **1a** are stable at −40 °C for hours and can therefore be spectroscopically characterized.

Complexes **3**, **3a** and **3b** each contain a high-spin Fe^{III} ion in an octahedral *fac*-N_3O_3 donor set. The CV of **3a** is shown in Figure 8. Three reversible one-electron oxidation waves and, in addition, a reversible one-electron reduction at a very negative

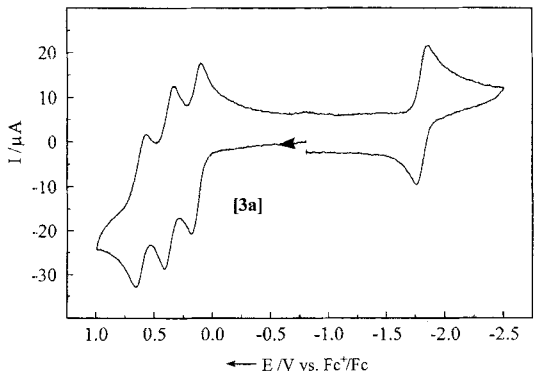

Figure 8. Cyclic voltammogram of **3a** in CH_3CN (conditions as given in Figure 6).

potential are observed. The latter process is assigned to a metal-centred reduction of Fe^{III} to Fe^{II}, whereas the three oxidation waves are ligand-centred successive phenoxyl radical formation processes. In this instance, the mono- and dications are stable in solution and can readily be prepared by coulometry. The CV of **3** is similar, but the third oxidation process leading to the trication is irreversible, and the CV of **3b** displays only irreversible oxidation processes, indicating that the phenoxyl radicals are not stable under these conditions. Interestingly, both **3** and **3b** display a *reversible* one-electron metal-centred reduction wave at quite negative potentials ($E^4_{1/2}$; Table 3). These reduction waves of **3**, **3a** and **3b** have similar redox potentials. The three coordinated phenolato groups enormously stabilize the +III oxidation state of the central iron ion. This is a general feature of phenolato iron complexes.

In the potential range +0.70 to −1.5 V vs Fc^+/Fc the CV's of **4′** and **4b** each display two reversible one-electron transfer processes [Eq. (3)], which are assigned to the metal-centred cou-

$$[Mn^{IV}L]^- \underset{+e}{\overset{-e(E^4)}{\rightleftharpoons}} [Mn^{III}L] \underset{+e}{\overset{-e(E^5)}{\rightleftharpoons}} [Mn^{II}L]^- \qquad (3)$$

ples Mn^{IV}/Mn^{III} and Mn^{III}/Mn^{II} ($E^4_{1/2}$ and $E^5_{1/2}$ in Table 3), respectively. The CV's of **4b** and **4b′** are identical. Note that **4b** and **4b′** have been isolated as solids and were fully characterized as high-spin Mn^{III} and Mn^{IV} complexes, respectively.

The square-wave voltammogram of $[Mn^{IV}L^{OCH_3}]PF_6$ (**4a′**) is shown in Figure 9, where the expanded potential range +1.5 to −2.5 V vs Fc^+/Fc has been scanned. The two metal-centred reversible one-electron transfer processes E^4 and E^5 have very similar redox potentials to the above complexes **4′** and **4b** (**4b′**) and are assigned to the couples Mn^{IV}/Mn^{III} (E^4) and Mn^{III}/Mn^{II} (E^5). In addition, three further oxidative processes were detected, two of which, E^1 and E^2, at 0.89 and 0.74 V are irreversible, but the third E^3 at 0.56 V vs Fc^+/Fc is *reversible* and corresponds to a one-electron oxidation of the $[Mn^{IV}L^{OCH_3}]^+$ species to a dication, as was indicated by a coulometric measurement. Spectroelectrochemistry provides evidence (see below) that this oxidation is ligand-centred rather than metal-centred.

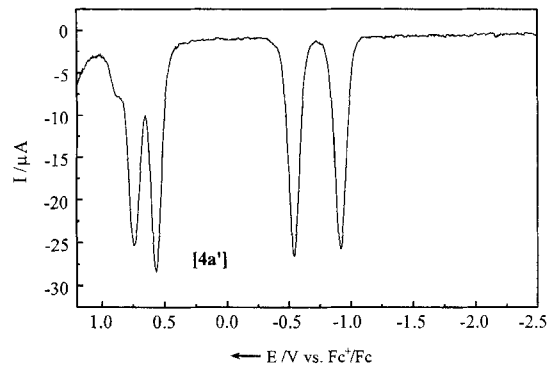

Figure 9. Square-wave voltammogram of **4a′** in CH_3CN (0.10 M $[N(nBu)_4]PF_6$): other conditions as in Figure 7.

The difference between the redox potentials E^1, E^2 and E^3 of a given species is nearly constant irrespective of the nature of the coordinated central metal ion (Figure 10). A very simple electrostatic model that takes into account only the difference in solvation energy of species carrying an n^+ and an $(n+1)^+$ charge has been developed by using the Born equation for a charged spherical particle of radius r in a medium with dielectric constant ε_E [Eq. (4)], where E^f is the redox potential in V, N_L

$$-\Delta G^\circ = E^f F = n^2 e^2 N_L / 8\pi r \varepsilon_o \varepsilon_E \qquad (4)$$

is the Avogadro number, F is the Faraday constant, $8\pi r$ is a geometric parameter of the spherical particle, $\varepsilon_o\varepsilon_E$ is the dielectric constant of the surrounding medium and ne is the electric charge of the particle. Assuming that the difference of the redox potentials $[LM]^{n+/(n+1)+}$ ($n = 0, 1, 2$) is primarily governed by the differing solvation energies of the two charged species one can derive Equation (5).

$$\Delta E^f = (2n-1)(e^2 N_L / 8\pi r \varepsilon_o \varepsilon_E) F^{-1} \qquad (5)$$

This simple model predicts that a plot of the measured redox potentials for a given complex $[LM]^n$ versus $2n-1$ should be linear with a slope $k = (e^2 N_L / 8\pi r \varepsilon_o \varepsilon_E) F^{-1}$. As Figure 10 shows, this is indeed the case. Note that the slopes k for the series **1a**, **2a**, **3a** are nearly identical (105, 105, 122 mV, respectively), irrespective of the nature of the coordinated metal ion. Most importantly, a very similar k (83 mV) is observed for the oxidations of $[\mathbf{4a'}]^+$ to $[\mathbf{4a'}]^{2+}$, to $[\mathbf{4a'}]^{3+}$ and to $[\mathbf{4a'}]^{4+}$ (if one

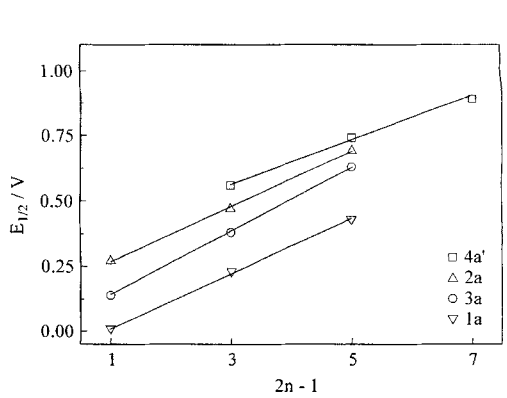

Figure 10. Dependence of the redox potentials $E^1_{1/2}$, $E^2_{1/2}$, $E^3_{1/2}$ of the couples $[LM]^{n+}/[LM]^{(n-1)+}$ on $2n$-1 where n represents the charge of the species $[LM]^n$. The solid lines are for guidance only.

0947-6539/97/0302-0312 $ 15.00+.25/0 Chem. Eur. J. 1997, 3, No. 2

assumes that the E_p^{ox} values for the $[\mathbf{4a'}]^{2+/3+}$ and $[\mathbf{4a'}]^{3+/4+}$ couples represent the $E_{1/2}^{x}$ values of the oxidation processes). This is again interpreted as a clear indication that oxidation of the manganese(IV) species **4a'** to the dication $[\mathbf{4a'}]^{2+}$ is a ligand-centred process, as are the two further oxidation steps.

If one now considers the fact that all [LM] complexes (M = Co^{III},[16] Cr^{III},[13] Fe^{III}, Ga^{III}, Sc^{III}) are isostructural and that one-electron oxidation is ligand-centred in all cases, it is somewhat surprising that the redox potential $E_{1/2}^3$ (and similarly $E_{1/2}^2$ and $E_{1/2}^1$) for the ligand oxidation is rather strongly metal ion dependent. Thus, $E_{1/2}^3$ for the couple $[LM]^{+/0}$ is −0.10 V vs Fc^+/Fc for the cobalt(III) complex[16] but +0.27 V vs Fc^+/Fc for the scandium(III) complex **2a**. The oxidizability of the coordinated phenolate ligands is obviously dependent on the nature of the metal ion to which it is bound. If the t_{2g} orbitals of the metal ion are unoccupied or only half-filled, the $M-O_{phenolate}$ bond has partial double-bond character due to phenolate-to-metal π-donation. As a relative measure for the strength of the covalent $M-O_{phenolate}$ bond we calculate the difference Δ between the sum of the effective ionic radii of the metal(III) ion and an O^{2-} ion[17] and the experimentally determined $M-O_{phenolate}$ bond length. The larger Δ is, the more covalent is the $M-O_{phenolate}$ bond and thus π-donor bonding prevails. As shown in Figure 11, a clear correlation exists between Δ, representing the π-donor strength, and the redox potential $E_{1/2}^3$ exists. Strong $M-O_{phenolate}$ π-donor bonding renders ligand oxidation more difficult (Sc represents an extreme case), whereas weakly π-accepting metal ions facilitate radical formation (Co^{III} with a filled t_{2g} subshell is the other extreme).

It is well established that the $O_{phenolate}-M-O_{phenolate}$ bond angle α in a *fac*-N_3O_3M octahedron also represents a measure for the degree of $M=O_{phenolate}$ double-bond formation: α is approximately 90° for $M-O_{phenolate}$ single bonds and increases with increasing $M=O_{phenolate}$ double-bond character.[7a,b] The inset in Figure 11 shows that a linear correlation exists between the redox potential $E_{1/2}^3$ and this α.

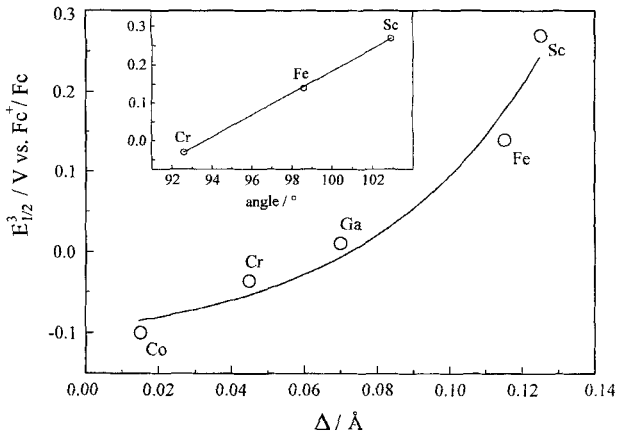

Figure 11. Dependence of the redox potentials $E_{1/2}^3$ of the couple $[LM]^{+/0}$ on the difference Δ [(ionic radius: $M^{n+} + O^{2-}$) − (experimental $M-O_{phenolate}$)]. The inset shows the dependence of the redox potential $E_{1/2}^3$ on the $O_{phenolate}-M-O_{phenolate}$ angle α.

4. Electronic spectra: The ligands $L^{Bu}H_3$, $L^{OCH_3}H_3$ and $L^{CH_3}H_3$, dissolved in acetonitrile, each display two π–π* transitions of the phenol pendent arms [$L^{Bu}H_3$: 226 nm ($\varepsilon = 1.5\times10^4$ L mol^{-1} cm^{-1}), 283 (7.2×10^3); $L^{OCH_3}H_3$: 233 (1.8×10^4), 295 (1.3×10^4); $L^{CH_3}H_3$: 219 (8.7×10^3), 286 (3.3×10^3)]. Upon coordination to Ga^{III} or Sc^{III} (complexes **1**, **1a**, **2**, **2a**, **2b**) these two absorption maxima undergo a slight bathochromic shift (Table 4). In CH_3CN the spectra of the yellow-green monooxidized forms of these complexes, generated electrochemically at controlled potentials (or in solution of [**1a**]ClO_4), also display these two UV absorption maxima but, in addition, three maxima in the visible: two intense bands between 390 and 430 nm ($\varepsilon > 10^3$ L mol^{-1} cm^{-1}) and a transition at 600–800 nm of much lower intensity (100–600 L mol^{-1} cm^{-1}). These new transitions are characteristic of phenoxyl radicals.[18] The spectrum of 2,4,6-tri-*tert*-butylphenoxyl has been reported: 625 nm ($\varepsilon \approx 400$ L mol^{-1} cm^{-1}), 400 (1.8×10^3), 382 (1.5×10^3).[19]

Table 4. UV/Vis spectral data and magnetic properties of complexes in CH_3CN.

Complex	λ_{max} [nm] (ε [L mol^{-1} cm^{-1}])	μ_{eff} [μ_B] [d]	S_t
1	248 (2.5×10^4), 296 (8.4×10^3)	dia	0
[**1**]$^+$ [b]	243 (1.8×10^4), 296 (1.2×10^4), 394 sh (2.1×10^3), 410 (2.7×10^3), 781 (230)	n.m.	1/2
1a	245 (2.0×10^4), 307 (1.1×10^4)	dia	0
[**1a**]ClO_4	246 (1.4×10^4), 310 (1.5×10^4), 340 sh (4.3×10^3), 408 sh (4.3×10^3), 427 (5.2×10^3), 600 (192)	1.73	1/2
[**1a**]$^{2+}$ [a]	243 (1.3×10^4), 313 (1.8×10^4), 333 sh (1.3×10^4), 417 sh (7.2×10^3), 432 (8.9×10^3),	n.m.	?
[**1a**]$^{3+}$ [a]	243 (1.3×10^4), 315 (2.1×10^4), 333 sh (1.6×10^4), 420 (9.8×10^3), 436 (1.3×10^4)	n.m.	?
2	252 (4.0×10^4), 292 (8.3×10^3)	dia	0
[**2**]$^+$ [b]	250 (2.7×10^4), 294 (1.3×10^4), 413 (3.1×10^3), 827 (220)	n.m.	1/2
2a	253 (4.2×10^4), 307 (1.3×10^4)	dia	0
[**2a**]$^+$ [b]	253 (1.8×10^4), 308 (1.2×10^4), 411 sh (3.6×10^3), 432 (4.2×10^3), 618 (178)	n.m.	1/2
2b	247 (3.9×10^4), 296 (9.7×10^3)	dia	0
3	244 (2.5×10^4), 287 (1.8×10^4), 330 sh (1.0×10^4), 500 (8.4×10^3)	5.9	5/2
[**3**]$^+$ [b]	248 sh (1.5×10^4), 298 (1.4×10^4), 344 (7.5×10^3), 406 (4.6×10^3), 564 (4.8×10^3)	n.m.	?
3a	245 (2.2×10^4), 303 (2.1×10^4), 513 (8.9×10^3)	5.9	5/2
[**3a**]ClO_4	241 (2.0×10^4), 302 (2.2×10^4), 332 sh (1.2×10^4), 402 sh (7.8×10^3), 421 (1.0×10^4), 562 (6.7×10^3)	4.9	2
[**3a**]$^{2+}$ [b]	244 (2.0×10^4), 300 (2.2×10^4), 332 (1.4×10^4), 431 (1.8×10^4), 610 (6.5×10^3), 750 sh (5.0×10^3)	n.m.	?
3b	243 (2.4×10^4), 290 (1.6×10^4), 320 sh (7.0×10^3), 486 (8.5×10^3)	5.8	5/2
4'	276 (1.7×10^4), 439 (7.3×10^3), 634 (6.3×10^3)	3.9	3/2
4a'	236 (2.3×10^4), 295 (2.4×10^4), 332 sh (7.9×10^3), 445 (8.0×10^3), 678 (7.8×10^3)	3.9	3/2
[**4a'**]$^{2+}$ [c]	239 (2.0×10^4), 288 (2.1×10^4), 320 sh (1.0×10^4), 441 (9.5×10^3), 720 (5.6×10^3)	n.m.	?
4b	246 (2.8×10^4), 295 (1.8×10^4), 379 (4.8×10^4), 650 (950)	4.7	2
4b'	277 (2.1×10^4), 416 (8.2×10^3), 612 (7.9×10^3)	3.8	3/2

[a] Species generated coulometrically at −30 °C in CH_3CN (0.10 M $[N(nBu)_4]PF_6$) from the corresponding neutral trisphenolato complex. [b] Species generated as above at 22 °C. [c] Species generated coulometrically at −30 °C in CH_3CN (0.10 M $[N(nBu)_4]PF_6$) from **4a'**. [d] n.m. = not measured; dia = diamagnetic.

Lippard et al.[2] have characterized the phenoxyl radical 1,1-bis-(2-(1-methylimidazolyl)-1-(3,5-di-*tert*-butyl-4-oxyphenyl)ethane and reported its spectrum in CH_3CN: 638 nm (ε = 430 $L\,mol^{-1}\,cm^{-1}$), 394 (1700), 378 (1500). Electrochemical generation of the dication $[\mathbf{1a}]^{2+}$ by controlled potential coulometry at −30 °C produced a green solution, the spectrum of which also shows these three transitions (Table 4; Figure 12) in the visible, with increased intensity. We take this as an indication that a second phenolate pendent arm of the coordinated ligand is oxidized, generating a second phenoxyl radical. The trication $[\mathbf{1a}]^{3+}$ was generated similarly, and its spectrum is shown in Figure 12. It displays the same transitions, with again with increased intensity in the visible. This indicates that all three pendent phenolato arms in **1a** undergo successive one-electron oxidation up to three coordinated phenoxyl radicals in $[\mathbf{1a}]^{3+}$. Thus, the electronic spectra of $[\mathbf{1}]^+$, $[\mathbf{1a}]^+$, $[\mathbf{1a}]^{2+}$, $[\mathbf{1a}]^{3+}$, $[\mathbf{2}]^+$ and $[\mathbf{2a}]^+$ all show the typical transitions of phenoxyl radicals (Table 4).

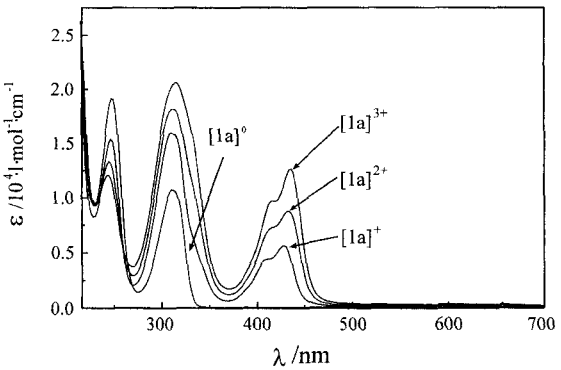

Figure 12. Electronic spectra of **1a** and electrochemically generated $[\mathbf{1a}]^+$, $[\mathbf{1a}]^{2+}$ and $[\mathbf{1a}]^{3+}$ in CH_3CN (0.10 M $[N(n-Bu)_4]PF_6$).

The spectra of the neutral iron complexes **3**, **3a** and **3b** show an intense and characteristic phenolate-to-iron(III) charge transfer (CT) band in the visible (≈500 nm) and the two $\pi-\pi^*$ transitions of the coordinated phenolates in the ultraviolet region. A shoulder at ≈330 nm is tentatively assigned to an amine-to-iron CT band. One-electron oxidation of **3** and **3a** produces the stable monocations $[\mathbf{3}]^+$ and $[\mathbf{3a}]^+$, and in the case of **3a** the electrochemically generated dication $[\mathbf{3a}]^{2+}$ is stable enough at 22 °C to allow its electronic spectrum to be measured.

Figure 13 shows the spectra of **3a**, $[\mathbf{3a}]^+$ and $[\mathbf{3a}]^{2+}$, the solutions of which are red, blue and green, respectively. Since the spectra of **3** and **3a** show an absorption minimum at ≈400 nm it is significant that the oxidized species $[\mathbf{3}]^+$ and $[\mathbf{3a}]^+$ both display a new intense asymmetric maximum in this region. We take this as a fingerprint of the formation of a phenoxyl radical rather than a metal-centred oxidation to Fe^{IV}. It is also significant that this maximum has approximately twice the intensity in $[\mathbf{3a}]^{2+}$ as compared to its monocation $[\mathbf{3a}]^+$; this indicates the presence of two phenoxyl radicals in $[\mathbf{3a}]^{2+}$. Interestingly, these one-electron oxidations of **3** and **3a** cause a bathochromic shift of the phenolate-to-iron CT band and its intensity decreases.

The spectra of the manganese(IV)-containing species $[\mathbf{4'}]PF_6$, $[\mathbf{4a'}]PF_6$ and $[\mathbf{4b'}]_2(ClO_4)_3(H_2O)_3(H_3O)$ are similar in the visible and display two intense ($\varepsilon > 10^3$ $L\,mol^{-1}\,cm^{-1}$) phenolato-to-manganese(IV) CT bands at ≈420 and ≈650 nm.[7] Electrochemical one-electron oxidation of $[\mathbf{4a'}]PF_6$ in acetonitrile solution at −30 °C produces a stable dication $[\mathbf{4a'}]^{2+}$, the spectrum of which is shown in Figure 14. Owing to the fact that this oxidation diminishes the intensity of the CT band of $[\mathbf{4a'}]^+$ at 678 nm and shifts its maximum to 720 nm, whereas the band at 450 nm ($[\mathbf{4a'}]^+$) gains in intensity and shifts to a shorter wavelength at 441 nm, we assume this oxidation to be ligand- rather than metal-centred with formation of a phenoxyl radical rather than an Mn^V species.

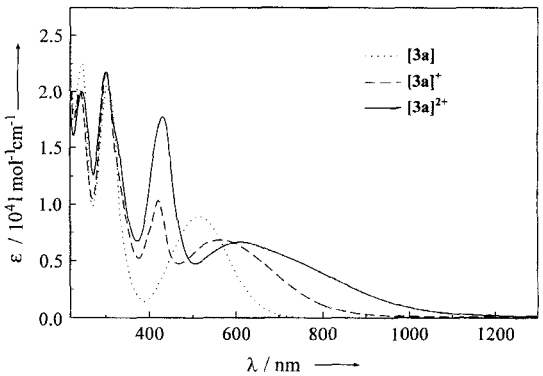

Figure 13. Electronic spectra of **3a**, $[\mathbf{3a}]ClO_4$ and electrochemically generated $[\mathbf{3a}]^{2+}$ in CH_3CN.

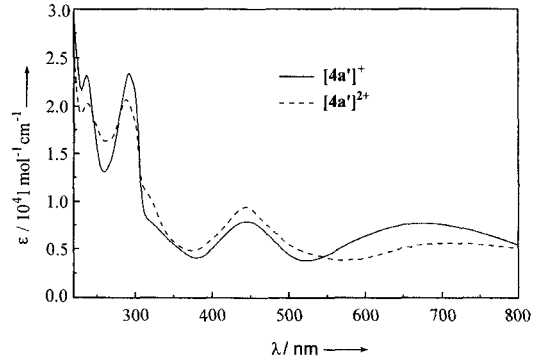

Figure 14. Electronic spectra of $[\mathbf{4a'}]PF_6$ and electrochemically generated $[\mathbf{4a'}]^{2+}$ in CH_3CN (0.10 M $[N(n-Bu)_4]PF_6$).

5. Magnetic properties of complexes: The temperature-dependence of the molar magnetic susceptibility of solid samples of complexes was studied on a SQUID magnetometer in the range 2–300 K. Experimental susceptibilities were corrected for underlying diamagnetism by use of Pascal's tabulated constants. Magnetic moments are summarized in Table 4.

The colourless or pale yellow neutral species **1**, **1a**, **2**, **2a** and **2b** are diamagnetic as judged by their ^1H NMR spectra (see Experimental Section). The neutral iron(III)-containing complexes **3**, **3a** and **3b** have a temperature-independent magnetic moment of 5.9 μ_B, indicating a high-spin d^5 electronic configuration ($S = 5/2$). Complex $[\mathbf{1a}]ClO_4$ is paramagnetic with a temperature-independent magnetic moment of 1.7 μ_B ($S = 1/2$) in the range 10–300 K.

The temperature-dependence of the magnetic moment of $[\mathbf{3a}]ClO_4$ is more complex and is shown in Figure 15. μ_{eff} de-

0947-6539/97/0302-0314 $ 15.00+.25/0 Chem. Eur. J. 1997, 3, No. 2

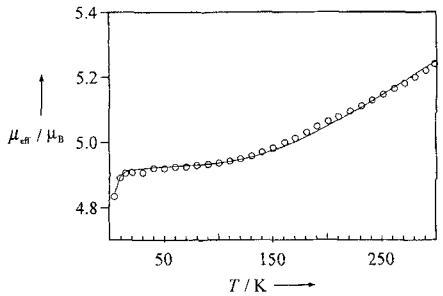

Figure 15. Temperature dependence of the magnetic moment, μ_{eff}/μ_B, of [**3a**]ClO_4. The solid line represents a best fit to the spin Hamiltonian $H = -2JS_1 \cdot S_2$ ($S_1 = 5/2$; $S_2 = 1/2$) (see text).

creases monotonically from 5.25 μ_B at 300 K to a plateau value of 4.9 μ_B below 100 K, which remains constant to ≈10 K. This indicates an $S = 2$ ground state. The temperature-dependence was readily modelled by using the isotropic Heisenberg–Dirac–van Vleck (HDvV) spin-coupling model [$H = -2JS_1S_2 + g\mu_B B(S_1 + S_2)$) for a high-spin iron(III) ion ($S_1 = 5/2$) coupled to a phenoxyl radical ($S_2 = 1/2$). The following numerical values were obtained from a fitting procedure to the above spin-Hamiltonian: $J = -80\ cm^{-1}$, $g = 2.0$ (fixed), and a small amount of [**3a**] (1.6%) as paramagnetic impurity with $S = 5/2$. The intramolecular antiferromagnetic exchange coupling then gives the observed $S = 2$ ground state. The result proves that the phenoxyl radical is coordinated to the iron(III) ion, because in Lippard's model such antiferromagnetic coupling does not exist in a complex with an uncoordinated phenoxyl radical.[2]

Complex **4b** exhibits a temperature-independent magnetic moment of 4.7 μ_B (80–300 K), indicative of an octahedral high-spin manganese(III) ion. Its oxidized form $[\mathbf{4b}']_2(ClO_4)_3(H_2O)_3(H_3O)$ displays an effective magnetic moment of 3.86 μ_B per manganese ion, in agreement with its formulation as an Mn^{IV} ion (d^3). Complexes [**4′**]PF_6 and [**4a′**]PF_6 also have a temperature-independent magnetic moment of 3.9 μ_B (10–300 K). In all these cases, metal-centred oxidation states of III or IV prevail.

6. Mössbauer spectra: Zero-field Mössbauer spectra of **3**, **3a** and **3b** have been recorded at 80 K. The isomer shifts δ of 0.49, 0.50 and 0.48 $mm\,s^{-1}$ vs α-Fe at 298 K and the small quadrupole splitting ΔE_Q of 0.83, 0.60 and 0.76 $mm\,s^{-1}$ for **3**, **3a** and **3b**, respectively, clearly indicate the presence of highly symmetric (octahedral), high-spin iron(III) ions in these complexes.[20] Most importantly, the Mössbauer spectrum of [**3a**]ClO_4 at 5 K also shows a single quadrupole doublet with $\delta = 0.54\ mm\,s^{-1}$ and $\Delta E_Q = 0.95\ mm\,s^{-1}$. Thus, one-electron oxidation of [**3a**] does not induce a significant change in the isomer shift δ and, consequently, the oxidation cannot be metal-centred. Fe^{IV} complexes have very small or even negative isomer shifts ($\delta = -0.1$ to $-0.29\ mm\,s^{-1}$).[20] [**3a**]ClO_4 also contains a high-spin iron(III) ion. The increased quadropole splitting in [**3a**]$^+$ as compared to [**3a**] may indicate a lower symmetry of the ligand field in the oxidized complex. This may be interpreted as evidence for a localized coordinated phenoxyl radical ligand at 5 K (on the timescale of a Mössbauer experiment: $\approx 10^{-7}$ s) in [**3a**]$^+$ giving rise to an N_3FeO_2O' donor set of C_{2v} symmetry.

7. EPR-spectra: X-band EPR spectroscopy on acetonitrile solutions of the electrochemically generated monocations [**1**]$^+$ and [**2**]$^+$ and of their benzyl-deuterated forms [D_6-**1**]$^+$ and [D_6-**2**]$^+$ proved to be very informative concerning the question as to whether the phenoxyl radical is coordinated to the metal ion gallium(III) and scandium(III). Figure 16 shows these spectra.

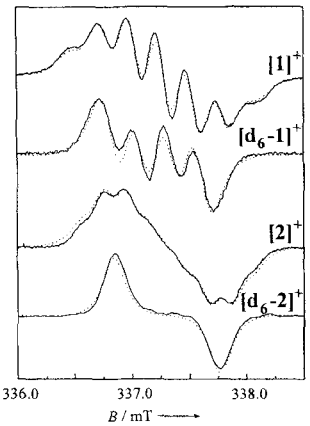

Figure 16. X-band EPR spectra of electrochemically generated [**1**]$^+$, [D_6-**1**]$^+$, [**2**]$^+$ and [D_6-**2**]$^+$ in CH_3CN (0.10 M [$N(nBu)_4$]PF_6) at 298 K (conditions: 9.4592 GHz, 0.45 mW; modulation frequency: 100 kHz; modulation amplitude: 0.026 mT). Solid lines represent experimental spectra, broken lines are simulations using the parameters in Table 5. The ordinates are in arbitrary units of dX″/dB.

All four species display a signal at 298 K with hyperfine structure at $g = 2.0041 \pm 0.0002$, which is characteristic for phenoxyl radicals.[18] The spectra were satisfactorily simulated by taking into account of the hyperfine coupling with the gallium ($^{71/69}Ga$, nuclear spin $I = 3/2$) or the scandium ion (^{45}Sc, $I = 7/2$), as well as of three equivalent protons of the ligand. The simulation parameters are listed in Table 5. Since the form of these signals responds to the selective deuteration of the six benzylic protons ($a_H/a_D \approx 6.5$), coupling to one of the diastereotopic protons of each of the three benzyl groups must occur. This immediately implies that on the EPR timescale ($\approx 10^{-8}$ s) at ambient temperature the unpaired electron in [**1**]$^+$ and [**2**]$^+$ is delocalized over all three phenolate groups. Note that this is probably not the case for [**3a**]$^+$ where Mössbauer spectroscopy (see above) may imply the presence of one localized phenoxyl radical (timescale $\approx 10^{-7}$ s) at 5 K. The large hyperfine coupling to the gallium or scandium ion proves conclusively that the phenoxyl radical is coordinated and not dangling as in Lippard's model complex.[2]

Table 5. EPR simulation parameters.

	a_{metal} [mT] [a]	a_H (3 H) [mT] [a] a_D (3 D) [mT]	$\Delta\nu_{1/2}$ [mT] [b]
[**1**]$^+$	0.230 (^{69}Ga) 0.290 (^{71}Ga)	0.230	0.155
[D_6-**1**]$^+$	0.230 (^{69}Ga) 0.290 (^{71}Ga)	0.035	0.120
[**2**]$^+$	0.117 (^{45}Sc)	0.207	0.140
[D_6-**2**]$^+$	0.117 (^{45}Sc)	0.032	0.104

[a] Hyperfine coupling constants. [b] Line width at half height.

Discussion

We have recently published the syntheses and crystal structures of blue [$L^{OCH_3}Cr^{III}$]·$2CH_3CN$ and its violet one-electron oxidized form [$L^{OCH_3}Cr^{III}$]ClO_4·$3CH_3CN$.[13] The former has a temperature-independent magnetic moment of 3.87 μ_B indicative of an $S = 3/2$ ground state of a chromium(III) complex,

whereas for the latter a temperature-independent μ_{eff} of 2.83 μ_B indicates an $S = 1$ ground state of the monocation, which is attained by strong intramolecular antiferromagnetic coupling between a coordinated phenoxyl radical ($S = 1/2$) and a chromium(III) ion ($S = 3/2$). In the crystal structure of $[L^{OCH_3}Cr^{III}]ClO_4$, the phenoxyl radical and the two phenolate pendant arms of the macrocyclic ligand are clearly discernible and agree with the two differing resonance structures shown in Figure 17.

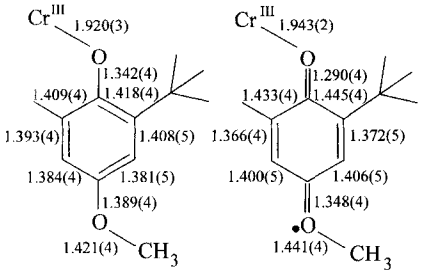

Figure 17. Structural data of $[Cr^{III}L^{OCH_3}]ClO_4 \cdot 3\,CH_3CN$ [13]. On the left-hand side the average bond lengths of the two coordinated phenolate pendent arms are given, and on the right-hand side those for the coordinated phenoxyl radical, for which one resonance structure is drawn.

The two phenolates and the phenoxyl radical are coordinated to the metal ion. Interestingly,the $Cr-O_{phenoxyl}$ bond length of 1.943(2) Å is slightly longer than the $Cr-O_{phenolate}$ bond length of 1.920(3) Å. In contrast, in the trianionic triscatecholatochromium(III) complex,[21] $[CrL_3]^{3-}$, where L is 3,5-di-*tert*-butylcatecholate(2 −), the average $Cr-O_{cat}$ bond length is 1.986(4) Å, whereas in its oxidized form,[22] $[CrL'_3]$ [L' = 3,5-di-*tert*-butylsemiquinonate(1 −)], the $Cr-O_{semiquinone}$ distance is shorter at 1.933(5) Å. Complexes of this type have been shown to undergo reversible or quasi-reversible one-electron redox steps to give Cr(quinone)$^n_3$, where n ranges from 3 + to 3 − .[23] Thus, coordinated tris(O-catecholates) display a similar chemistry[24] to the phenolato complexes reported here.

From EPR and susceptibility measurements[13] we have concluded that the electronic ground states of the neutral complex $[L^{OCH_3}Cr^{III}]$ is $S = 3/2$, that of the monocation is $S = 1$, that of the dication is $S = 1/2$ and that of the trication is $S = 0$. These ground states are attained *via* intramolecular antiferromagnetic exchange coupling between zero, one, two or three coordinated phenoxyl radicals and a central chromium(III) (t^3_{2g}) ion.

Similarly, the corresponding neutral iron complexes **3**, **3a** and **3b** contain high-spin iron(III) ions with $S = 5/2$ ground states, whereas the corresponding monocations have $S = 2$. For the dications $S = 3/2$ and for the trication $S = 1$ ground states are expected, but this has not yet been proven experimentally. This behaviour is again in excellent agreement with that of analogous tris(catecholato)iron(III) complexes[25] and their semiquinonate analogues, which have recently been shown by high magnetic field Mössbauer spectroscopy[25c] to exhibit relatively localized bonding between a high-spin ferric ion and semiquinonate radical ligands.

In the neutral trisphenolate complexes containing redox-inactive gallium(III) or scandium(III) ions, the monooxidized forms $[\mathbf{1}]^+$, $[\mathbf{1a}]^+$, $[\mathbf{2}]^+$ and $[\mathbf{2a}]^+$ contain one coordinated phenoxyl radical. The EPR spectra of $[\mathbf{1a}]^+$ and $[\mathbf{2a}]^+$ in acetonitrile solution at room temperature show that the unpaired electron is delocalized over the whole cation on the EPR timescale ($\approx 10^{-8}$ s). It is interesting to note that in tris(semi-quinonato)gallium(III) complexes the spins of the three unpaired electrons are aligned parallel,[26] giving rise to an $S = 3/2$ ground state. Ferromagnetic intramolecular coupling of this kind operating through superexchange mechanisms has also been observed for metal(IV) derivatives of the dinegative radical ligand 3,5-di-*tert*-butyl-1,2-semiquinonato-1-(2-hydroxy-3,5-di-*tert*-butylphenyl)imine (M^{IV} = Ti, Ge, Sn).[27] We therefore expect similar behaviour for the present di- and trications, which should yield $S = 1$ and $S = 3/2$ ground states.

All the available spectroscopic data suggest that the oxidized forms of LM^{III} complexes (M = Ga, Sc, Cr, Fe) contain coordinated phenoxyl radicals. In no instance has a metal-centred oxidation been observed. The situation is different for the manganese complexes; the monocations $[\mathbf{4'}]^+$, $[\mathbf{4a'}]^+$ and $[\mathbf{4b'}]^+$ clearly containing a manganese(IV) ion. The spectroelectrochemical investigation of the dication $[\mathbf{4a'}]^{2+}$ then points to a ligand-centred oxidation. This species is most probably a manganese(IV) complex with a coordinated phenoxyl radical. Intramolecular antiferromagnetic coupling is expected to yield an $S = 1$ ground state in $[\mathbf{4a'}]^{2+}$.

The chemistry described in this paper places coordinated phenolates in the growing class of noninnocent organic ligands such as 1,2-dithiolenes, diimines, quinones and porphyrins. We have, therefore, checked the recent literature for first-row transition metal complexes with "unusually" high oxidation states of the central metal ion and coordinated phenolates. In a series of interesting papers, Koikawa, Okawa, Kida et al.[28–31] have described octahedral complexes of "Mn^V", "Fe^{IV}" and "Co^{IV}". In addition, they have described dinuclear copper(II) complexes which they show to undergo a one-electron oxidation to the mixed valent "$Cu^{II}Cu^{III}$" and a further one-electron oxidation to a dinuclear "Cu^{III}_2" species. These complexes contain, in their reduced forms, trianionic ligands derived from *N*-(2-hydroxyphenyl)salicylamide. The mononuclear bis-complexes $[M^{III}L_2]^{3-}$ (M = Fe, Co) and a $[Mn^{IV}L_2]^{2-}$ species were subjected to one-electron oxidation by use of Ce^{IV} to give $[ML_2]^{2-}$ and an $[MnL_2]^-$ species. In our view, all the spectroscopic data and the magnetochemistry reported by these authors are also compatible with formulation as $M^{III}-\dot{O}R$ (M = Co^{III}, Fe^{III}) and $Mn^{IV}-\dot{O}R$ species. Similarly, the $Cu^{III}-OR$ complexes may in fact be $Cu^{II}-\dot{O}R$. In all these cases, strong intramolecular antiferromagnetic coupling of the d^n electrons with the radical spin would give the observed ground states. A similar case has recently been reported by Collins et al.[32] for an iron(III) complex containing a similar coordinated radical ligand.[32] It is not a trivial matter to characterize the electronic structure of such complexes.

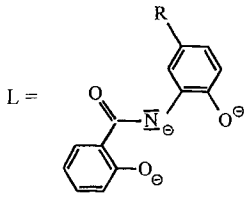

R = H, CH_3, Cl, NO_2

Recently, Tolman et al. have reported a mononuclear copper(II) complex that contains a coordinated phenoxyl radical.[34] This complex serves as a structural model for the enzyme galactose oxidase.

0947-6539/97/0302-0316 $ 15.00+.25/0 Chem. Eur. J. 1997, 3, No. 2

Experimental Section

1,4,7-Tris(3,5-dimethyl-2-hydroxybenzyl)-1,4,7-triazacyclononane ($L^{CH_3}H_3$) [9]: A solution of 1,4,7-triazacyclononane (tacn) (3.0 g, 0.024 mol) and paraformaldehyde (2.16 g, 0.072 mol) in methanol (100 mL) was refluxed for 0.5 h. 2,4-Dimethylphenol (9.0 g, 0.074 mol) was added to the orange solution. The mixture was refluxed for 12 h and allowed to cool to room temperature. The white product was collected by filtration. Yield: 7.6 g (60%); ^{1}H NMR (400 MHz, $CDCl_3$, 20 °C): δ = 2.20, 2.25 (s, 3H, s, 3H, PhCH_3), 2.85 (s, 4H, NCH_2CH_2N), 3.70 (s, 2H, NCH_2Ph), 6.60 (s, 1H, PhH), 6.95 (s, 1H, PhH), 9.95 (brs, 1H, PhOH); ^{13}C NMR (100.62 MHz, $CDCl_3$, 293 K): δ = 15.4, 20.6 (CH_3), 55.3 (NCH_2CH_2N), 62.4 (NCH_2Ph), 121.1, 124.5, 127.1, 127.7, 130.9 (arom. C), 153.0 (arom. COH); MS (FAB): m/z (%): 532.8 (100) [M+H$^+$]; $C_{33}H_{45}N_3O_3$ (531.74): calcd C 74.5, H 8.5, N 7.9, found C 74.8, H 8.8, N 7.3.

1,4,7-Tris(3,5-di-*tert*-butyl-2-hydroxybenzyl)-1,4,7-triazacyclononane ($L^{tBu}H_3$): A solution of tacn (1.0 g, 8 mmol) and paraformaldehyde (0.72 g, 0.042 mol) in methanol (20 mL) was refluxed for 2 h. 2,4-Di-*tert*-butylphenol (9.8 g, 0.048 mol) and a few drops of conc. HCl were added to the orange solution. The mixture was refluxed for 3 h and allowed to cool to room temperature. The white product was isolated by filtration and recrystallized from acetonitrile solution. Yield: 3.1 g (50%); ^{1}H NMR (400 MHz, $CDCl_3$, 293 K): δ = 1.24, 1.42 (s, 9H, s, 9H, PhC(CH_3)$_3$), 2.82 (s, 4H, NCH_2CH_2N), 3.71 (s, 2H, NCH_2Ph), 6.75, 7.21 (d, 1H, d, 1H, ^4J(H,H) = 2.34 Hz, PhH), 10.1 (brs, 1H, PhOH); ^{13}C NMR (100.62 MHz, $CDCl_3$, 293 K): δ = 28.8, 31.8 (C(CH_3)$_3$), 34.2, 34.9 (C(CH$_3$)$_3$), 55.4 (NCH_2CH_2N), 63.5 (NCH_2Ph), 121.5, 123.5, 123.8, 135.7, 141.0 (arom. C), 154.0 (arom. COH); MS (FAB): m/z (%): 784.6 (100) [M^+]; $C_{51}H_{81}N_3O_3$ (784.2): calcd C 78.1, H 10.4, N 5.4, found C 78.7, H 11.4, N 5.4.

1,4,7-Tris(3-*tert*-butyl-5-methoxy-2-hydroxybenzyl)-1,4,7-triazacyclononane ($L^{OCH_3}H_3$): The same procedure as described for $L^{tBu}H_3$ was employed, but 2-*tert*-butyl-4-methoxy-phenol (8.7 g, 0.048 mol) was used. Yield: 2.8 g (50%); ^{1}H NMR (270 MHz, $CDCl_3$, 300 K): δ = 1.40 (s, 9H, PhC(CH_3)$_3$), 2.79 (s, 4H, NCH_2CH_2N), 3.67 (s, 2H, NCH_2Ph), 3.69 (s, 3H, OCH_3), 6.32, 6.79 (d, 1H, d, 1H, ^4J(H,H) = 2.91 Hz, PhH), 9.83 (brs, 1H, PhOH); ^{13}C NMR (67.93 MHz, $CDCl_3$, 293 K): δ = 29.4 (C(CH$_3$)$_3$), 34.8 (C(CH$_3$)$_3$), 55.4 (NCH$_2$$CH_2$N), 55.6 (O$CH_3$), 63.2 (NCH$_2$Ph), 111.3, 113.1 (arom. CH), 122.7 (arom. CC(CH$_3$)$_3$), 138.0 (arom. CCH$_2$N), 150.0, 151.9 (arom. COH and arom. COCH$_3$); MS (ESIp): m/z (%): 706.0 (72) [M+H^+]; $C_{42}H_{63}N_3O_6$ (705.98): calcd C 71.5, H 9.0, N 6.0, found C 71.4, H 9.1, N 6.0.

1,4,7-Tris(3,5-di-*tert*-butyl-2-deuterohydroxybenzyl)-1,4,7-triazacyclononane ([D$_6$]-$L^{tBu}D_3$): The same procedure as described for $L^{tBu}H_3$, but CH_3OD, $(CD_2O)_n$ and conc. DCl in D_2O were used. The ^{1}H NMR spectrum exhibits the same signals as reported for $L^{tBu}H_3$ except for the signals for the benzylic and phenolic protons; MS (EIp): m/z (%): 789 (80) [D$_6$-$L^{tBu}H_3$]$^+$, 790 (100) [D$_6$-$L^{tBu}D_1H_2$]$^+$, 791 (70) [D$_6$-$L^{tBu}D_2H_1$]$^+$, 792 (25) [D$_6$-$L^{tBu}D_3$]$^+$; $C_{51}H_{72}D_9N_3O_3$ (793.15): calcd C 78.1, H 10.4, N 5.4, found C 78.7, H 10.4, N 5.4. The deuterated ligand [D$_6$]-$L^{OCH_3}D_3$ was prepared analogously.

All following manipulations were carried out under an argon atmosphere in water-free solvents.

1: $GaCl_3$ (0.17 g, 1 mmol) was added to a solution of $L^{tBu}H_3$ (0.78 g, 1 mmol) in acetonitrile (30 mL). After refluxing for 2 h and cooling to room temperature, a white microcrystalline product formed and was collected by filtration. Yield: 0.39 g (46%); ^{1}H NMR (400 MHz, $CDCl_3$, 300 K): δ = 1.16, 1.24 (s, 9H, s, 9H, PhC(CH_3)$_3$), 2.60, 2.80, 3.40 (m, 1H, m, 2H, m, 1H, NCH_2CH_2N), 3.55, 4.90 (d, 1H, d, 1H, ^2J(H,H) = 12.50 Hz, NCH_2Ph), 6.63, 7.12 (d, 1H, d, 1H, ^4J(H,H) = 2.59 Hz, PhH); ^{13}C NMR (100.26 MHz, $CDCl_3$, 293 K): δ = 30.1, 31.9 (C(CH$_3$)$_3$), 34.0, 35.1 (C(CH$_3$)$_3$), 49.3, 53.5 (NCH$_2$$CH_2$N), 64.1 (NCH$_2$Ph), 117.3 (arom. CCH$_2$N), 123.0, 122.2 (arom. CH, 135.0, 137.8, (arom. CC(CH$_3$)$_3$), 160.5 (arom. COGa); MS (FAB): m/z (%): 850.0 (100) [M^+]; $C_{51}H_{78}N_3O_3Ga$ (850.9): calcd C 72.0, H 9.2, N 4.9, found C 69.8, H 9.3, N 4.8.

1a: $GaCl_3$ (0.17 g, 1 mmol) was added to a solution of $L^{OCH_3}H_3$ (0.71 g, 1 mmol) in acetonitrile (30 mL). After refluxing for 2 h and cooling to room temperature, a white microcrystalline product formed which was isolated by filtration. Yield: 0.42 g (55%); ^{1}H NMR (270 MHz, CD_2Cl_2, 300 K): δ = 1.31 (s, 9H, PhC(CH_3)$_3$), 2.55, 2.80, 3.11 (m, 1H, m, 2H, m, 1H, NCH_2CH_2N), 3.40, 4.70 (d, 1H, d, 1H, ^2J(H,H) = 12.58 Hz, NCH_2Ph), 3.69 (s, 3H, OCH_3), 6.31, 6.78 (d, 1H, d, 1H, ^4J(H,H) = 3.12 Hz, PhH); ^{13}C NMR (100.62 MHz, CD_2Cl_2, 300 K): δ = 30.0 (C(CH_3)$_3$), 35.4 (C(CH$_3$)$_3$), 49.0, 56.1 (NCH$_2$$CH_2$N), 55.2 (O$CH_3$), 64.3 (NCH$_2$Ph), 112.1, 113.9 (arom. CH), 118.7 (arom. CC(CH$_3$)$_3$), 140.1 (arom. CCH$_2$N), 148.7 (arom. COCH$_3$), 158.4 (arom. COGa); MS (ESIp) m/z (%): 772.0 (50), 774.0 (40) [M+H]$^+$; $C_{42}H_{60}N_3O_6Ga$ (772.68): calcd C 65.3, H 7.8, N 5.4, found C 64.8, H 7.7, N 5.6.

[1a]ClO$_4$: [Ni^{III}(tacn)$_2$](ClO$_4$)$_3$ [14] (0.62 g, 1 mmol) was added to a solution of **1a** (0.77 g, 1 mmol) in CH_3CN (45 mL) at −18 °C. After stirring for 15 min. the green solution was filtered, and the solvent partly removed by rotary evaporation under reduced pressure. A green solid precipitated and was collected by filtration. Yield: 0.40 g (46%); MS (ESIp) m/z (%): 756.5 (69), 758.5 (52) [M^+ − ClO$_4$ − OCH$_3$]; 771.5 (100), 773.5 (74), [M^+ − ClO$_4$]; $C_{42}H_{60}N_3O_{10}ClGa$ (872.13): calcd C 57.8, H 6.9, N 4.8, ClO$_4$ 11.4, found C 57.0, H 6.9, N 4.5, ClO$_4$ 11.0.

2: $ScCl_3 \cdot 6H_2O$ (0.26 g, 1 mmol) was added to a solution of $L^{tBu}H_3$ (0.78 g, 1 mmol) in acetonitrile (30 mL). After refluxing for 2 h and cooling to room temperature, a white microcrystalline product formed, which was isolated by filtration. Yield: 0.36 g (44%); ^{1}H NMR (400 MHz, CD_3CN, 300 K): δ = 1.26, 1.41 (s, 9H, s, 9H, PhC(CH_3)$_3$), 2.38, 2.75, 3.05 (m, 2H, m, 1H, m, 1H, NCH_2CH_2N), 3.31, 4.03 (d, 1H, d, 1H, ^2J(H,H) = 12.23 Hz, NCH_2Ph), 6.95, 7.22 (d, 1H, d, 1H, ^4J(H,H) = 2.49 Hz, PhH); ^{13}C NMR (100.61 MHz, CD_3CN, 300 K): δ = 30.2, 32.1 (C(CH$_3$)$_3$), 34.6, 35.6 (C(CH$_3$)$_3$), 49.5, 59.0 (NCH$_2$$CH_2$N), 64.4 (NCH$_2$Ph), 124.4 (arom. CCH$_2$N), 124.7, 126.4 (arom. CH), 136.2, 137.7 [arom. CC(CH$_3$)$_3$], 161.7 (arom. COSc); $C_{51}H_{78}N_3O_3Sc$ (826.2): calcd C 74.2, H 9.5, N 5.1, found C 74.8, H 9.3, N 5.0.

[D$_6$]-1 and **[D$_6$]-2**: The same procedures as described for **1** and **2** were employed, but [D$_6$]-$L^{tBu}D_3$ was used. The ^{1}H NMR spectra show the same signals as reported for **1** and **2**, except for the signals of the benzylic protons; MS (ESIp): m/z (%): 832 (100) [M^+]; $C_{51}H_{72}D_6N_3O_3Sc$ (832.2).

2a: $ScCl_3 \cdot 6H_2O$ (0.26 g, 1 mmol) was added to a solution of $L^{OCH_3}H_3$ (0.71 g, 1 mmol) in acetonitrile (30 mL). After refluxing for 2 h and cooling to room temperature, a white crystalline product formed which was isolated by filtration. Yield: 0.46 g (62%); ^{1}H NMR (400 MHz, $CDCl_3$, 300 K): δ = 1.41 (s, 9H, PhC(CH_3)$_3$), 2.30, 2.58, 2.84 (m, 1H, m, 1H, m, 2H, NCH_2CH_2N), 3.15, 4.19 (d, 1H, d, 1H, ^2J(H,H) = 12.15 Hz, NCH_2Ph), 3.72 (s, 3H, OCH_3), 6.46, 6.84 (d, 1H, d, 1H, ^4J(H,H) = 3.15 Hz, PhH); ^{13}C NMR (100.62 MHz, $CDCl_3$ 300 K): δ = 29.5 [C(CH$_3$)$_3$], 35.0 [C(CH$_3$)$_3$], 49.0, 58.4 (NCH$_2$$CH_2$N), 55.8 (O$CH_3$), 64.0 (NCH$_2$Ph), 112.8, 113.6 (arom. CH), 123.0 (arom. CC(CH$_3$)$_3$), 138.2 (arom. CCH$_2$N), 148.8 (arom. COCH$_3$), 157.6 (arom. COSc); MS (ESIp) m/z (%): 747.0 (100) [M^+]; $C_{42}H_{60}N_3O_6Sc$ (747.97): calcd C 67.5, H 8.1, N 5.6, found C 68.0, H 8.0, N 5.6.

2b: A few drops of NEt_3 were added to a solution of $L^{CH_3}H_3$ (0.54 g, 1 mmol) and $ScCl_3 \cdot 6H_2O$ (0.26, 1 mmol) in acetonitrile (30 mL). After refluxing for 3 h and cooling to room temperature, a white microcrystalline product formed which was isolated by filtration. Crystals of **2b**·2CH_3CN were obtained by recrystallization from CH_3CN. Yield: 0.41 g (72%); ^{1}H NMR (400 MHz, $CDCl_3$, 293 K): δ = 2.15, 2.18 (s, 3H, s, 3H, PhCH_3), 2.20, 2.58, 2.81 (m, 1H, m, 1H, m, 2H, NCH_2CH_2N), 3.21, 4.33 (d, 1H, d, 1H, ^2J(H,H) = 14.13 Hz, NCH_2Ph), 6.68, 6.90 (d, 1H, d, 1H, PhH); ^{13}C NMR (100.62 MHz, $CDCl_3$, 293 K): δ = 14.5, 19.4 (CH_3), 49.2, 58.3 (NCH$_2$$CH_2$N), 61.8 (NCH$_2$Ph), 120.9, 122.7, 124.5, 127.3, 130.5 (arom. C), 159.0 (arom. COSc); MS (FAB): m/z (%): 573.20 (100) [M^+]; $C_{33}H_{42}N_3O_3Sc$ (573.7): calcd C 69.1, H 7.4, N 7.3, found C 69.5, H 7.6, N 7.1.

3: $FeCl_3 \cdot 9H_2O$ (0.52, 1 mmol) was added to a solution of $L^{tBu}H_3$ (0.78 g, 1 mmol) in methanol (50 mL). The solution was refluxed for 0.5 h. NEt_3 (1 mL) was added to the violet solution, and the resulting red solution was refluxed for 2 h. After cooling to room temperature, water (5 mL) was added, which initiated the precipitation of a microcrystalline red solid. Yield: 0.70 g (83%); MS (FAB): m/z (%): 836.5 (100) [M^+]; $C_{51}H_{78}N_3O_3Fe$ (837.1): calcd C 73.2, H 9.4, N 5.0, found C 71.3, H 9.5, N 4.9.

3a: The same procedure as described for **3** was employed, but $L^{OCH_3}H_3$ (0.71 g, 1 mmol) was used. Yield: 0.48 (63%); MS (ESIp) m/z (%): 759.0 (100) [M^+]; $C_{42}H_{60}N_3O_6Fe$ (758.8): calcd C 66.5, H 8.0, N 5.5, Fe 7.4, found C 66.8, H 8.0, N 5.4, Fe 7.2.

[3a]ClO$_4$: [Ni^{III}(tacn)$_2$](ClO$_4$)$_3$ (0.62 g, 1 mmol) was added to a solution of **3a** (0.76 g, 1 mmol) in CH_3CN (45 mL) at −18 °C. After 15 min the blue solution was filtered, and the solvent was partly removed by evaporation under

reduced pressure. The deep blue microcrystalline solid was isolated by filtration. Yield: 0.48 g (56%); MS (ESIp) *m/z* (%): 758.5 (100) $[M^+]$; $C_{42}H_{60}N_3O_{10}ClFe$ (858.3): calcd C 58.8, H 7.1, N 4.9, Fe 6.5, ClO_4 11.6, found C 58.5, H 6.8, N 5.1, Fe 6.3, ClO_4 11.3.

3b: NEt_3 (1 mL) was added to a solution of $L^{CH_3}H_3$ (0.53 g, 1 mmol) and $FeCl_3 \cdot 9H_2O$ (0.52, 1 mmol) in acetone (30 mL). After 1 h of stirring, water (5 mL) was added, which initiated the precipitation of a microcrystalline red solid. Yield: 0.43 (73%); MS (FAB) *m/z* (%): 583.1 (100) $[M^+]$; $C_{33}H_{45}N_3O_3Fe$ (584.6): calcd C 67.7, H 7.3, N 7.2, found C 68.2, H 8.0, N 7.2.

4': A solution of $[Mn^{III}_3O(CH_3CO_2)_6]CH_3CO_2$ (0.23 g, 0.33 mmol) and $L^{Bu}H_3$ (0.79 g, 1 mmol) in acetone (30 mL) was refluxed in the presence of air for 0.5 h. After addition of a few drops of NEt_3 and heating for 2 h, a deep green solution formed. $NaPF_6$ (0.5 g, 3 mmol) was added to the cooled (20 °C) solution, and $[L^{Bu}Mn^{IV}]PF_6$ was isolated as a green solid by filtration. Yield: 0.77 g (78%); MS (FAB) *m/z* (%): 835.6 (100) $[M^+ - PF_6]$; $C_{51}H_{78}N_3O_3MnPF_6$ (981.1): calcd C 62.4, H 8.0, N 4.3, found C 61.3, H 8.6, N 3.8.

4a': The same procedure as described for **4'** was employed, but $L^{OCH_3}H_3$ (0.71 g, 1 mmol) was used. Yield: 0.60 g (67%); MS (ESIp) *m/z* (%): 757.0 (100) $[M^+ - PF_6]$; $C_{42}H_{60}N_3O_6MnPF_6$ (902.9): calcd C 55.9, H 6.7, N 4.7, Mn 6.1, found C 55.7, H 6.8, N 4.7, Mn 6.0.

4b: A solution of $L^{CH_3}H_3$ (0.53 g, 1 mmol) and $[Mn^{III}_3O(CH_3CO_2)_6]CH_3CO_2$ (0.23 g, 0.33 mmol) in acetone (30 mL) was heated to reflux for 0.5 h. NEt_3 (2 mL) was added, and the solution heated for 2 h. Water (6 mL) was added to the green solution, which initiated the precipitation of a microcrystalline green solid. Yield 0.54 g (93%); MS (FAB) *m/z* (%): 583.1 (100) $[M^+]$; $C_{33}H_{42}N_3O_3Mn$ (583.7): calcd C 67.9, H 7.3, N 7.1, found C 68.2, H 7.5, N 6.8.

$[4b']_2(ClO_4)_3(H_3O)(H_2O)_3$: **4b** (0.59 g, 1 mmol) was dissolved in methanol in the presence of air and $HClO_4$ (60%, 0.5 mL) was added. After 3 d in an open vessel, deep green crystals precipitated. Yield: 0.35 g, (23%); MS (FAB) *m/z* (%): 583.2 (100) $[M^+ - ClO_4]$; $C_{66}H_{96}N_6O_{22}Mn_2Cl_3$ (1538.8): calcd C 51.5, H 6.1, N 5.2, found C 50.1, H 6.1, N 5.2.

Physical Measurements: Electronic spectra of the complexes and spectra of the spectroelectrochemical investigations were recorded on a Perkin Elmer Lambda 19 (range: 220–1400 nm) and on a HP 8452A diode array spectrophotometer (range: 220–820 nm), respectively. Cyclic voltammograms, square-wave voltammograms and coulometric experiments were performed on EG & G equipment (Potentiostat/Galvanostat Model 273A). EPR spectra of complexes (10^{-3} M, CH_3CN solution containing 0.10 M $[N(nBu)_4]PF_6$) were measured at 298 K in a quartz cell (d = 0.3 mm). The data were digitized on a data station (Stelar s.n.c., Mede, Italy). The spectra were simulated by iteration of the isotropic hyperfine coupling constants and line widths a and $\Delta v_{1/2}$. We thank Dr. F. Neese (Abteilung Biologie der Universität Konstanz) for a copy of his EPR simulation program. Temperature-dependent (2–298 K) magnetization data were recorded on a SQUID magnetometer (MPMS Quantum Design) in an external magnetic field of 1.0 T. The experimental susceptibility data were corrected for underlying diamagnetism by use of tabulated Pascal's constans. The Mössbauer spectra were recorded on an alternating constant-accelaration spectrometer. The source was $^{57}Co/Rh$ and the minimum experimental line width was 0.24 $mm\,s^{-1}$ full width at half maximum. The sample temperature was maintained constant in an Oxford Instruments Variox cryostat. Isomer shifts are quoted relative to iron metal at 300 K.

Crystal Structure Determinations: Details of the crystal data, data collection and refinement are summarized in Table 6. Intensities and lattice parameters of colourless crystals of $L^{Bu}H_3$, $L^{OCH_3}H_3$, **[2a]** and **[2b]**·$2CH_3CN$ were measured on an Enraf–Nonius CAD4 diffractometer by using $Cu_{K\alpha}$ radiation ($L^{Bu}H_3$, $L^{OCH_3}H_3$), and on a Siemens SMART system and a Siemens P4 diffractometer by using $Mo_{K\alpha}$ radiation for **[2a]** and **[2b]**·$2CH_3CN$, respectively. Similarly, a green crystal of **[4b]** $(CH_3OH)_2$ was studied on a Siemens P4 diffractometer by using $Mo_{K\alpha}$ radiation. No corrections for absorption effects were carried out. The structures were solved by conventional Patterson and difference Fourier and direct methods and refined with anisotropic thermal parameters for all non-hydrogen atoms. Neutral-atom scattering factors and anomalous dispersion corrections for non-hydrogen atoms were taken from ref. [33]. The Siemens programme package SHELXTL PLUS (G. M. Sheldrick, Universität Göttingen) was used throughout. All methyl, methylene and aromatic hydrogen atoms were placed at calculated positions and were refined with isotropic temperature factors. The function minimized during full-matrix least-squares refinement was $\sum w(|F_o| - |F_c|)^2$.

Further details of the crystal structure investigations may be obtained from the Fachinformationszentrum Karlsruhe, 76344 Eggenstein-Leopoldshafen (Germany) on quoting the depository number CSD-59362.

Received: September 18, 1996 [F456]

[1] Recent review articles: a) S. Erikson, B. M. Sjöberg, *Allosteric Enzymes* (Ed.: G. Herve), RC Press, Boca Raton, Florida, **1989**, 189–215; b) J. Stubbe, H. Eklund, P. Reichard, *Adv. Enzymol.* **1992**, *65*, 147; c) I. B. Vincent, G. L. Oliver-Lilley, B. A. Averill, *Chem. Rev.* **1990**, *90*, 1447.

[2] D. P. Goldberg, D. Koulougliotis, G. W. Brudvig, S. J. Lippard, *J. Am. Chem. Soc.* **1995**, *117*, 3134.

[3] a) G. Avigad, D. Amaral, C. Asensio, B. Horecker, *J. Biol. Chem.* **1962**, *237*, 2736; b) M. M. Whittaker, J. W. Whittaker, *ibid.* **1988**, *263*, 6074; *ibid.* **1990**, *265*, 9610; c) M. M. Whittaker, Y.-Y. Chuang, J. W. Whittaker, *J. Am. Chem. Soc.* **1993**, *115*, 10029; d) G. T. Babcock, M. K. El-Deeb, P. O. Sandusky, M. M. Whittaker, J. W. Whittaker, *ibid.* **1992**, *114*, 3727.

[4] a) N. Ito, S. E. Phillips, C. Stevens, Z. B. Orgel, M. J. McPherson, J. N. Keen, K. D. S. Yadav, P. F. Knowles, *Nature* **1991**, *350*, 87; b) P. F. Knowles, N. Ito

Table 6. Crystallographic data of ligands and complexes.

	$L^{Bu}H_3$	$L^{OCH_3}H_3$	**2a**	**[2b]**·$2CH_3CN$	**[4b]**$(CH_3OH)_2$
formula	$C_{51}H_{81}N_3O_3$	$C_{42}H_{63}N_3O_6$	$C_{42}H_{60}N_3O_6Sc$	$C_{37}H_{48}N_5O_3Sc$	$C_{35}H_{50}MnN_3O_5$
M_r	784.2	706.0	747.9	655.8	647.7
F_{000}	3456	3072	1608	700	692
crystal system	monoclinic	monoclinic	monoclinic	triclinic	triclinic
space group	$C2/c$	$C2/c$	$P2_1/n$	$P\bar{1}$	$P\bar{1}$
a [Å]	23.246(3)	27.116(1)	12.982(1)	11.683(2)	8.423(2)
b [Å]	18.572(2)	14.996(1)	20.363(3)	13.464(4)	11.852(2)
c [Å]	23.765(1)	21.109(1)	15.849(1)	13.563(4)	18.470(4)
α [°]				119.40(2)	96.92(3)
β [°]	101.19(1)	105.00(1)	99.660(7)	93.17(2)	102.89(3)
γ [°]				104.21(2)	108.29(3)
V [Å^3]	10065.1(6)	8290.9(6)	4130.3(14)	1762.6(8)	1670.3(8)
Z	8	8	4	2	2
d_c [g cm^{-3}]	1.03	1.13	1.203	1.236	1.288
μ ($Mo_{K\alpha}$) [mm^{-1}]	0.455	0.594	0.226	0.25	0.44
crystal size [mm]	0.21 × 0.35 × 0.49	0.43 × 0.65 × 0.48	0.46 × 0.53 × 0.14	0.3 × 0.24 × 0.18	0.49 × 0.5 × 0.15
collection T [K]	293	293	293	193	293
obs. unique reflns	9583	8532	9416	2334 [$F > 4.0\sigma(F)$]	3301 [$F > 4.0\sigma(F)$]
parameters refined	526	473	469	418	486
R [a]	0.074	0.044	0.049	0.070	0.042

[a] $R = \sum(|F_o| - |F_c|)/\sum|F_o|^2$.

0947-6539/97/0302-0318 $ 15.00+.25/0

in *Perspectives on Bioinorganic Chemistry* (Eds.: R. W. Hay, J. R. Dilworth, K. B. Nolan), JAI Press, London, **1993**, Vol. 2, p. 207.
[5] M. M. Whittaker, P. J. Kersten, N. Nakamura, J. Sanders-Loehr, E. S. Schweizer, J. W. Whittaker, *J. Biol. Chem.* **1996**, *271*, 681.
[6] D. P. Goldberg, S. J. Lippard, *Adv. Chem. Ser. 246* (Eds.: H. H. Thorp, V. L. Pecoraro), ACS, Washington D. C., **1995**, p. 61.
[7] a) U. Auerbach, U. Eckert, K. Wieghardt, B. Nuber, J. Weiss, *Inorg. Chem.* **1990**, *29*, 938; b) U. Auerbach, T. Weyhermüller, K. Wieghardt, B. Nuber, E. Bill, C. Butzlaff, A. X. Trautwein, *ibid.* **1993**, *32*, 508; c) U. Auerbach, S. P. C. Della Vedova, K. Wieghardt, B. Nuber, J. Weiss, *J. Chem. Soc. Chem. Commun.* **1990**, 1004.
[8] J. Hockertz, S. Steenken, K. Wieghardt, P. Hildebrandt, *J. Am. Chem. Soc.* **1993**, *115*, 11222.
[9] D. A. Moore, P. E. Fanwick, M. J. Welch, *Inorg. Chem.* **1989**, *28*, 1504.
[10] a) A. E. Martell, R. J. Motekaitis, M. J. Welch, *J. Chem. Soc. Chem. Commun.* **1990**, 1748; b) Y. Sun, H. L. Hu, A. E. Martell, A. Clearfield, *J. Coord. Chem.* **1995**, *36*, 23.
[11] E. T. Clarke, A. E. Martell, *Inorg. Chim. Acta* **1991**, *186*, 103.
[12] a) Y. Sun, A. E. Martell, J. H. Reibenspies, M. J. Welch, *Tetrahedron* **1991**, *47*, 357; b) R. J. Motekaitis, Y. Sun, A. E. Martell, *Inorg. Chim. Acta* **1992**, *198–200*, 421.
[13] A. Sokolowski, E. Bothe, E. Bill, T. Weyhermüller, K. Wieghardt, *Chem. Commun.* **1996**, 1671.
[14] a) K. Wieghardt, W. Schmidt, W. Hermann, H.-J. Küppers, *Inorg. Chem.* **1983**, *22*, 2953; b) K. Wieghardt, W. Walz, N. Nuber, J. Weiss, A. Ozarowski, H. Stratemeier, D. Reinen, *ibid.* **1986**, *25*, 1650.
[15] Preliminary results of the crystal structure determination of $[\mathbf{4b'}]_2(ClO_4)_3 \cdot (H_3O)(H_2O)_3$: $C_{33}H_{46}Cl_{1.5}MnN_3O_{11}$ (dark green), hexagonal space group $P6_3/m$, $a = 13.834(2)$, $c = 24.125(5)$ Å, $V = 3998.5(12)$ Å^3, $Z = 4$, $M_w = 763.8$, $\rho_{calcd} = 1.28$ g cm^{-3}, $\mu(Mo_{K\alpha}) = 0.486$ mm^{-1}, $T = 23\,^{\circ}C$, 1799 unique reflections $[F > 4.0\sigma(F)]$, refined parameters 169, $R(F) = 0.089$.
[16] The complex $[L^{OCH_3}Co^{III}]$ has been prepared and isolated as brown-green microcrystals. Details will be reported elsewhere.
[17] R. D. Shannon, *Acta Crystallogr.* **1976**, *A32*, 751.
[18] E. R. Altwicker, *Chem. Rev.* **1967**, *67*, 475.
[19] a) E. J. Land, G. Porter, *Trans. Farad. Soc.* (London), **1961**, *57*, 1885; b) E. J. Land, G. Porter, *Trans. Farad. Soc.* (London), **1963**, *59*, 2016.
[20] a) N. N. Greenwood, T. C. Gibb, *Mössbauer Spectroscopy*, Chapman and Hall, London, **1971**; b) U. Russo, G. J. Long in *Mössbauer Spectroscopy Applied to Inorganic Chemistry* (Eds.: G. J. Long, F. Grandjean), Plenum Press, New York, **1989**, Vol. 3.
[21] K. N. Raymond, S. S. Isied, L. D. Brown, F. R. Fronczek, J. H. Nibert, *J. Am. Chem. Soc.* **1976**, *98*, 1767.
[22] S. R. Sofen, D. C. Ware, S. R. Cooper, K. N. Raymond, *Inorg. Chem.* **1979**, *18*, 234.
[23] a) H. H. Downs, R. M. Buchanan, C. G. Pierpont, *Inorg. Chem.* **1979**, *18*, 1736; b) R. M. Buchanan, J. Claflin, C. G. Pierpont, *ibid.* **1983**, *22*, 2552.
[24] C. G. Pierpont, C. W. Lange, *Progr. Inorg. Chem.* **1994**, *41*, 331.
[25] a) R. M. Buchanan, S. L. Kessel, H. H. Downs, C. G. Pierpont, D. N. Hendrickson, *J. Am. Chem. Soc.* **1978**, *100*, 7894; b) M. W. Lynch, M. Valentine, D. N. Hendrickson, *ibid.* **1982**, *104*, 6982; c) M. J. Cohn, C.-L. Xie, J.-P. M. Tuchagues, C. G. Pierpont, D. N. Hendrickson, *Inorg. Chem.* **1992**, *31*, 5028; d) R. B. Lauffer, R. H. Heistand, L. Que, Jr., *ibid.* **1983**, *22*, 50.
[26] D. M. Adams, A. L. Rheingold, A. Dei, D. N. Hendrickson, *Angew. Chem.* **1993**, *105*, 434; *Angew. Chem. Int. Ed. Engl.* **1993**, *32*, 391.
[27] S. Bruni, A. Caneschi, F. Cariati, C. Delfs, A. Dei, D. Gatteschi, *J. Am. Chem. Soc.* **1994**, *116*, 1388.
[28] M. Koikawa, H. Okawa, S. Kida, *J. Chem. Soc. Dalton Trans.* **1988**, 641.
[29] M. Koikawa, M. Gotoh, H. Okawa, S. Kida, T. Kohzuma, *J. Chem. Soc. Dalton Trans.* **1989**, 1613.
[30] M. Koikawa, H. Okawa, Y. Maeda, S. Kida, *Inorg. Chim. Acta* **1992**, *194*, 75.
[31] M. Koikawa, H. Okawa, N. Matsumoto, M. Gotoh, S. Kida, T. Kohzuma, *J. Chem. Soc. Dalton Trans.* **1989**, 2089.
[32] M. J. Bartos, C. Kidwell, K. E. Kauffmann, S. W. Gordon-Wylie, T. J. Collins, G. C. Clark, E. Münck, S. T. Weintraub, *Angew. Chem.* **1995**, *107*, 1345; *Angew. Chem. Int. Ed. Engl.* **1995**, *34*, 1216.
[33] *International Tables for Crystallography*, Vol. IV, Kynoch, Birmingham, UK, **1974**, pp. 49 and 149.
[34] J. A. Halfen, V. G. Young, Jr., W. B. Tolman, *Angew. Chem.* **1996**, *108*, 1832; *Angew. Chem., Int. Ed. Engl.* **1996**, *35*, 1687.

Corrigendum: In the paper "Regiochemistry of Twofold Additions to [6,6] Bonds in C_{60}: Influence of the Addend-Independent Cage Distortion in 1,2-Monoadducts" (*Chem. Eur. J.* **1996**, *2*, 1537–1547), the labels in Figure 10 should read (clockwise from top, left) $HOMO_{cage}$, $HOMO_{cage}-1$, LUMO+1, and LUMO.